Environmental Science and Pollution Research (2022) 29:39860–39876
https://doi.org/10.1007/s11356-022-18969-7

RESEARCH ARTICLE

A stochastic approach for the assessment of suspended sediment concentration at the Upper Rhone River basin, Switzerland

Babak Vaheddoost[1] · Saeed Vazifehkhah[2] · Mir Jafar Sadegh Safari[3]

Received: 8 September 2021 / Accepted: 26 January 2022 / Published online: 3 February 2022

Abstract

This study addresses the link between suspended sediment concentration, precipitation, streamflow, and direct runoff components. This is important since suspended sediment concentration in the streamflow has invaluable importance in the management of the river basin. For this, the daily streamflow time series in five consecutive stations at Upper Rhone River Basin, a relatively large basin in the Alpine region of Switzerland, daily precipitation at one station, and the twice a week suspended sediment concentration records at the most downstream station between January 1981 and October 2020 are used. Initially, the base flow and the direct runoff associated with streamflow time series are obtained using the sliding interval method. Elasticity analyses between streamflow and suspended sediment concentration together with correlation, autocorrelation, partial autocorrelation, stationarity, and homogeneity are examined by the Augmented Dickey-Fuller and Pettitt's tests, respectively. Then, various stochastic scenarios are generated using the autoregressive moving average exogenous method (ARMAX). It is concluded that the precipitation and direct runoff have fewer effects on the suspended sediment concentration at downstream of the river. Hence, the cumulative effect of the glacier or snowmelt and channel erosion may exceed the effect of rain blown washouts on the suspended sediment concentration at the Port du Scex station. It is found that the ARMAX model results are satisfactory and can be suggested for further application.

Keywords Autoregressive moving average exogenous · Direct runoff · Streamflow · Suspended sediment · Upper Rhone basin

Introduction

The suspended sediment transport in the rivers is one of the significant factors which has a fundamental influence on hydraulic structures and is a key challenge for surface water exploitation (Kisi and Yaseen 2019). As an essential issue in the sediment transport process, the precise estimation of suspended sediment concentration (*SSC*) is compulsory for the design of hydraulic structures. In addition, the impact of the river's suspended sediment on the ecosystem, the pollution, and the quality of surface water resources gain a huge interest (e.g., Frings and Kleinhans 2008; Martinez et al. 2009; Shadkani et al. 2021; Shojaeezadeh et al. 2018; Samadianfard et al. 2021). The inaccurate estimation of *SSC* however leads to several unwanted impacts on the available resources, time, energy, and manpower (Meshram et al. 2021; Harun et al. 2021).

The management, measurement, and determining sediment transport process in the rivers are among the common subjects in sediment studies. Likewise, the deposition of sediment in the rivers is the most common phenomenal and costly challenge which could lead to considerable environmental, agricultural, and ecological problems. For instance, the sediment deposition in the dams would lower the active volume and increase its dead volume (Mohammadi et al.

Responsible Editor: Xianliang Yi

✉ Mir Jafar Sadegh Safari
jafar.safari@yasar.edu.tr

Babak Vaheddoost
babak.vaheddoost@btu.edu.tr

Saeed Vazifehkhah
svazifehkhah@wmo.int

[1] Department of Civil Engineering, Bursa Technical University, Bursa, Turkey

[2] Climate Services, World Meteorological Organization, Geneva, Switzerland

[3] Department of Civil Engineering, Yaşar University, Izmir, Turkey

2021). The *SSC* in rivers also has a significant impact on the drinking and agriculture water quality. For this, many scientists such as Jain (2001) believe that the association between the *SSC*, the water quality, and industrial water consumption needs to be determined prior to the advanced water resources planning and management. Also, Safari (2020) outlined that to discover the stochastic nature of sediment transport, the nonlinear attributes of its drivers and their contribution should be investigated through experimental and numerical studies.

By far, the application of time series analysis on sediment transport phenomena has been studied through different approaches (e.g., Andrews 1980; Walker and Hammack 2000; Wang et al. 2008; Yang et al. 2011). For instance, Tian et al. (2019) assessed the temporal and spatial variation of runoff and the *SSC* in the upper Yellow River, China. They depicted the abrupt changes within the applied variables of the post dam construction era, indicating an increase (decrease) in the runoff periodicities owing to the low (high) frequencies generated afterwards. Restrepo Lopez et al. (2017) examined the suspended sediment discharge variation and flux in Colombian Caribbean rivers using the wavelet spectrum. They revealed no significant trend on the *SSC*; however, the period 2000–2010 has the highest variations. Han et al. (2019) evaluated the precipitation-runoff-sediment transport relationship in the Wuding river basin in China using a long-term time series (1955–2012) and emphasized the drastic changes in the relationship of mentioned variables due to the several dam constructions along the river. Esteves et al. (2019) evaluated the probable links between rainfall discharge and suspended sediment transport during the flood events in a 20-km^2 mountainous Mediterranean catchment. The seasonality of suspended sediment concentration is emphasized and it was suggested that a minimum of 5 years of consecutive dataset is needed to define a reliable relationship among the applied variables. Zakwan et al. (2021) assessed the applicability of the magnitude performance analysis to derive the suspended sediment transport in the Drava river, Croatia. They found that by considering the discharge with a 1-year return interval, the annual maximum discharge transports about 90% of the total sediment concentration of the lower Drava River. Sok et al. (2021) analyzed the temporal variation of suspended sediment concentration in Cambodia's lower Mekong rivers and explained a decreasing trend over the period 1993–2018.

The sediment transport phenomena in the Rhone River (both in France and Switzerland) gained enormous attention in recent years. For instance, Stutenbecker et al. (2018) quantified the process of sediment generation and their spatial distribution in the Upper Rhone basin (URB) using various fingerprint techniques and pointed out that a considerable amount of glaciogenic sediments is currently linked to the retreating glaciers. From the geomorphological aspect, Schoch et al. (2018) tried to predict the location and spatial distribution of sediment and bedrock cover in the URB and revealed since the Little Ice Age, the amount of relative sediment cover has increased in de-glaciated areas. Costa et al. (2018b) assessed the changes in hydro-climatic drivers and suspended sediment at the Upper Rhone basin during 1975–2015. Their outcomes emphasized the dominance of erosive rainfall, ice melt, and snowmelt in the daily *SSC* prediction. They emphasized the need for analyzing the interactions between hydrological factors and sediment sources at URB in the future. Dabrin et al. (2021) assessed the suspended particulate matter transport at the Rhone basin (France) through different extraction methods including the fingerprinting method.

A literature survey indicates the lack of a study to examine a possible relationship between the total streamflow, direct runoff, and *SSC* in the URB. To this end, we have assessed the effect of rainfall washouts and sediments brought by direct precipitation over the Rhone River with sediments brought by the streamflow as a product of glacier or snow melts and channel erosion from the upstream. Then, by taking into consideration of the recent studies on *SSC* prediction at URB, this study aims to (i) evaluate the sediment concentration concerning direct runoff and streamflow in response to the monthly precipitation changes, and (ii) to conduct a multivariate stochastic approach in studying the suspended sediment concentration phenomenon at the URB.

Study area and data

The Upper Rhone basin (URB) is located between the Rhone Glacier and Lake Geneva in Switzerland with an approximate area of 5250 km^2. Its altitude varies between 372 and 4521 m with a mean of 2124 m, which hosts several peaks higher than 4000 m (Fig. 1). The Rhone River's watershed is a closed intra-montane which is one of the largest inner-orogeny watersheds in the European Alps that supplies around 75% of the total inflow and 85% of the supplied sediment to Lake Geneva (Loizeau et al. 2012; Klein 2016). The glacial erosion and mass wasting processes on steep hillslopes cause the supply and production of the sediment, which are largely controlled by precipitation, and snow and ice melt (Costa et al. 2018b). The URB was extensively influenced by anthropogenic impact. For instance, the Rhone River was channelized twice in the periods of 1863–1894

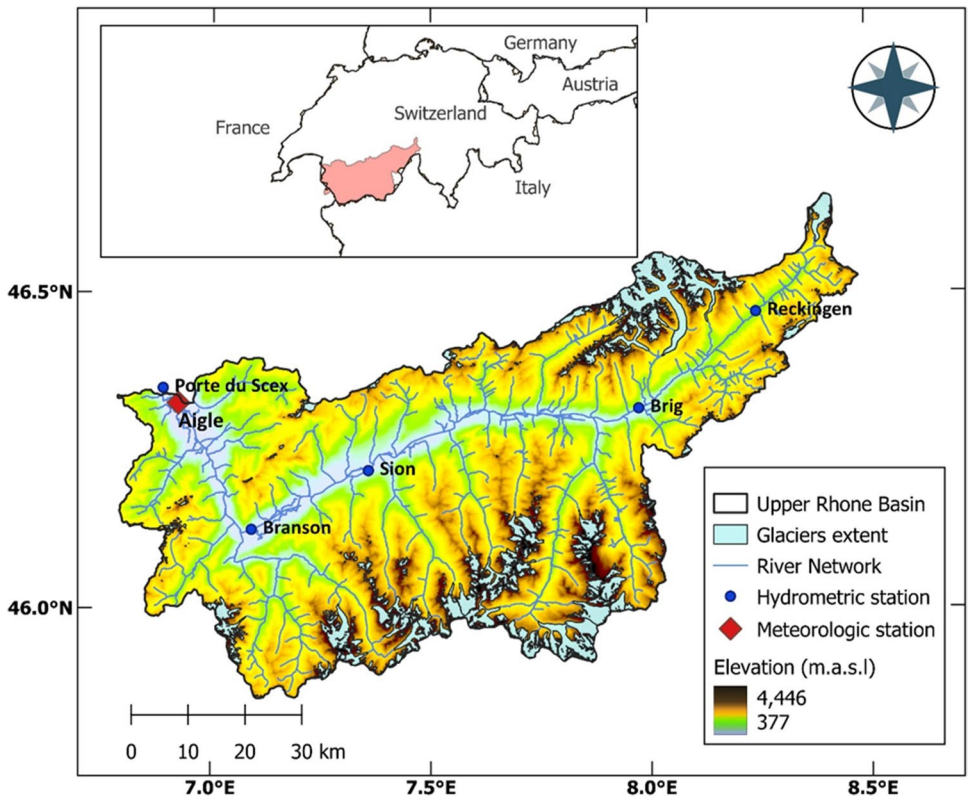

Fig. 1 Topographic map of the Upper Rhone basin with the applied gauging stations

and 1930–1960 at the downstream area continued by the ongoing 3rd Rhone Correction Project.

The annual mean precipitation in the URB is about 1400 mm with high spatial variability in response to the orographic effect (Costa et al. 2018a). The snowmelt and ice melt dominate the hydrological regime of the URB where the peak and low flows respectively take place in summer and winter. Mean discharge is about 320 m^3/s during June–August and 120 m^3/s during December–February, while the mean annual discharge is 181 m^3/s.

The daily precipitation (*P*) data at Aigle station; the daily discharge (*Q*) data at the Reckingen, Brig, Sion, Branson, and Porte du Scex stations which are consecutively located at the most upstream to most downstream of the Rhone river; and twice a week recorded SSC data at the Porte du Scex station were acquired from the Swiss Federal Office of the Environment (FOEN). In this regard, the selected stations

Table 1 General statistical and geographical information of the applied time series

ID	Station name	Average	Standard deviation	Frequency (unit)	Upstream area	Altitude	Glaciation %
P	Aigle	77.4	9.7	Daily (mm)	-	381	-
SSC	Porte du Scex	229.6	543.9	Twice a Week (mg/l)	-	377	-
*Q*1	Reckingen	9.8	9.6	Daily (m^3/s)	214	1311	12
*Q*4	Brig	42.0	43.1	Daily (m^3/s)	906	667	19
*Q*3	Sion	109.7	96.7	Daily (m^3/s)	3372	484	14
*Q*4	Branson	133.5	90.3	Daily (m^3/s)	3728	457	13
*Q*5	Porte du Scex	181.0	128.4	Daily (m^3/s)	5244	377	11

P, precipitation; *Q*, discharge; SSC, suspended sediment concentration

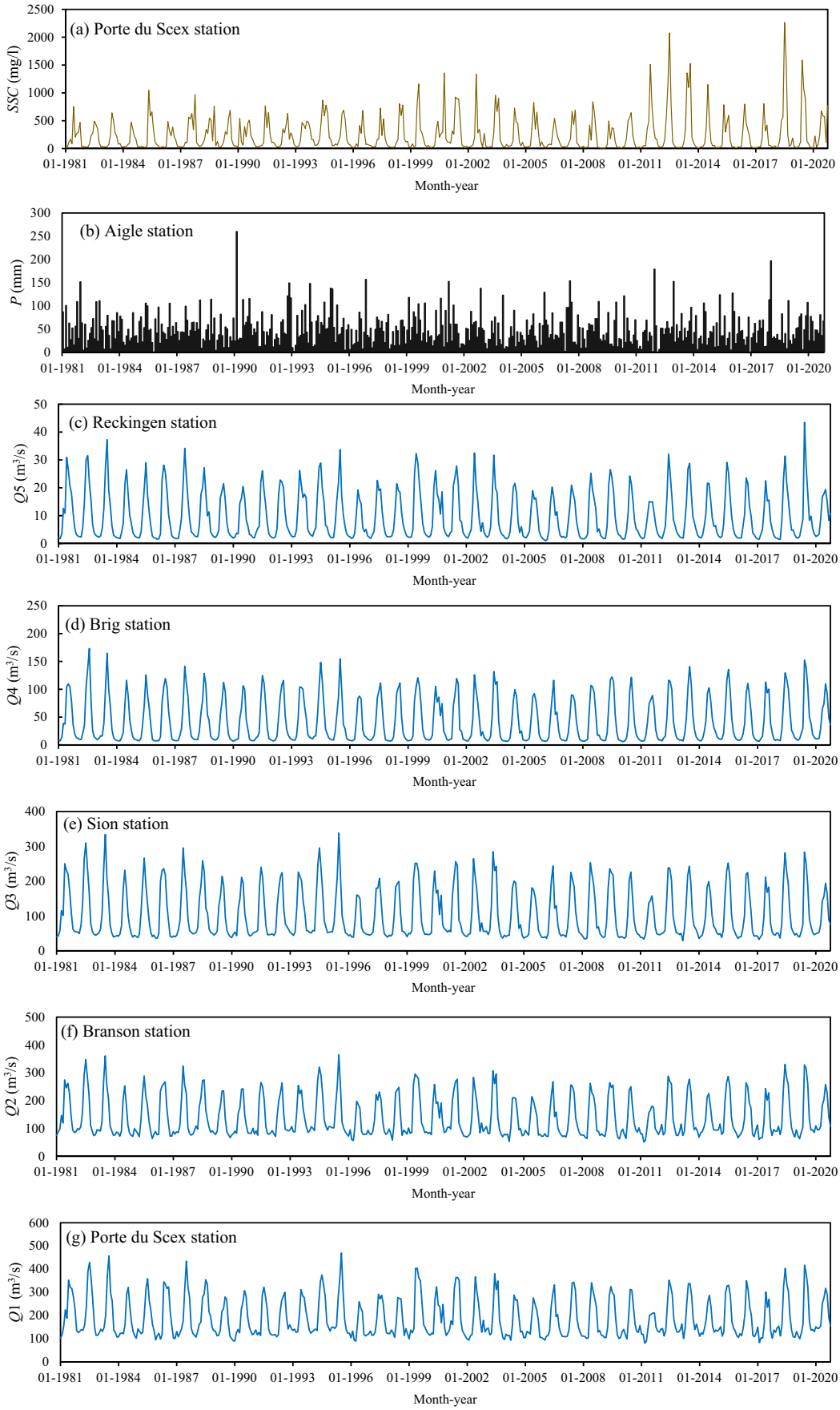
(a) Porte du Scex station
SSC (mg/l)
2500
2000
1500
1000
500
0
01-1981 01-1984 01-1987 01-1990 01-1993 01-1996 01-1999 01-2002 01-2005 01-2008 01-2011 01-2014 01-2017 01-2020
Month-year
(b) Aigle station
P (mm)
300
250
200
150
100
50
0
01-1981 01-1984 01-1987 01-1990 01-1993 01-1996 01-1999 01-2002 01-2005 01-2008 01-2011 01-2014 01-2017 01-2020
Month-year
(c) Reckingen station
Q5 (m³/s)
50
40
30
20
10
0
01-1981 01-1984 01-1987 01-1990 01-1993 01-1996 01-1999 01-2002 01-2005 01-2008 01-2011 01-2014 01-2017 01-2020
Month-year
(d) Brig station
Q4 (m³/s)
250
200
150
100
50
0
01-1981 01-1984 01-1987 01-1990 01-1993 01-1996 01-1999 01-2002 01-2005 01-2008 01-2011 01-2014 01-2017 01-2020
Month-year
(e) Sion station
Q3 (m³/s)
400
300
200
100
0
01-1981 01-1984 01-1987 01-1990 01-1993 01-1996 01-1999 01-2002 01-2005 01-2008 01-2011 01-2014 01-2017 01-2020
Month-year
(f) Branson station
Q2 (m³/s)
500
400
300
200
100
0
01-1981 01-1984 01-1987 01-1990 01-1993 01-1996 01-1999 01-2002 01-2005 01-2008 01-2011 01-2014 01-2017 01-2020
Month-year
(g) Porte du Scex station
Q1 (m³/s)
600
500
400
300
200
100
0
01-1981 01-1984 01-1987 01-1990 01-1993 01-1996 01-1999 01-2002 01-2005 01-2008 01-2011 01-2014 01-2017 01-2020
Month-year

◂**Fig. 2** Time series of (a) SSC at Porte du Scex station, (b) P at Aigle station together with the total streamflow in (c) Reckingen, (d) Brig, (e) Sion, (f) Branson, and (g) Porte du Scex stations

(Fig. 1) and the statistical properties of the data measured at each station are given in Table 1, which will be used through analysis in the subsequent sections. Although the period of acquired data varied among the streamflow stations, the common January 1981 to October 2020 time period between the allocated time series was chosen for further investigation. The statistical properties of the time series including average, standard deviation, frequency of records, drainage area, altitude, and glaciation extent are listed (Table 1). The time series plot of the raw data, initially provided for *P* and *SSC* (Fig. 2a, b) as well as the streamflow time series (*Q*) for the applied stations are presented (Fig. 2c–g).

Methods

The methodology used in this study consists of three main sections including; data regulation, data analysis and a mathematical simulation. Respectively, the subsequent sections detail the applied methods. First, the time series of suspended sediment concentration (*SSC*), streamflow (*Q*), and precipitation (*P*) are transformed into monthly time series (Fig. 3). The *Q* time series was converted to direct runoff (*DF*) and base flow (*BF*) time series to study the effect of precipitation. Then, the correlation analysis and sediment rating curves are obtained to study the spatial relationship between *SSC* and *Q* in the hydrometric stations and finally the allocated scenarios are used to generate the best simulation model using the Autoregressive Moving Average eXogenous (ARMAX) method. The procedure is shown in the flowchart given in Fig. 3.

Data regulation

The daily streamflow data were used to separate base flow and direct runoff to study the immediate effect of precipitation on the total streamflow on a daily time scale. For this, the base flow separation is conducted using the sliding interval method (Sloto and Crouse 1996) that determines the minimum streamflow discharge over half of the interval minus previous day streamflow [0.5(2 N*-1) days]. The sliding interval method can be illustrated with a moving bar 2 N* upward until it intersects with the daily streamflow hydrograph. The streamflow of any desired station is assigned to the median day within the assigned interval. Finally, the bar can be pushed over (being slid) to the next day and repeated over and over until the finalization of the procedure. Finally, each streamflow time series is evaluated as the total stream flow rate (*Q*), base flow (BF) separated with sliding interval method, and the direct runoff (*DR*) which is the residual between total streamflow and base flow time series at each interval (Fig. 4). According to the base flow separation analysis, more than 80% of the total streamflow in the river is the product of base flow. In order to clarify this issue, the base flow index (Vaheddoost and Aksoy 2018) as the percentage of ratio between *BF* to the *Q* is provided (Fig. 4).

Then, the daily precipitation data at the Aigle station and daily streamflow rate at Porte du Scex, Branson, Sion, Brig, and Reckingen stations, together with the daily suspended sediment concentration at the Porte du Scex station (refer to Table 1), are transferred respectively to the monthly average

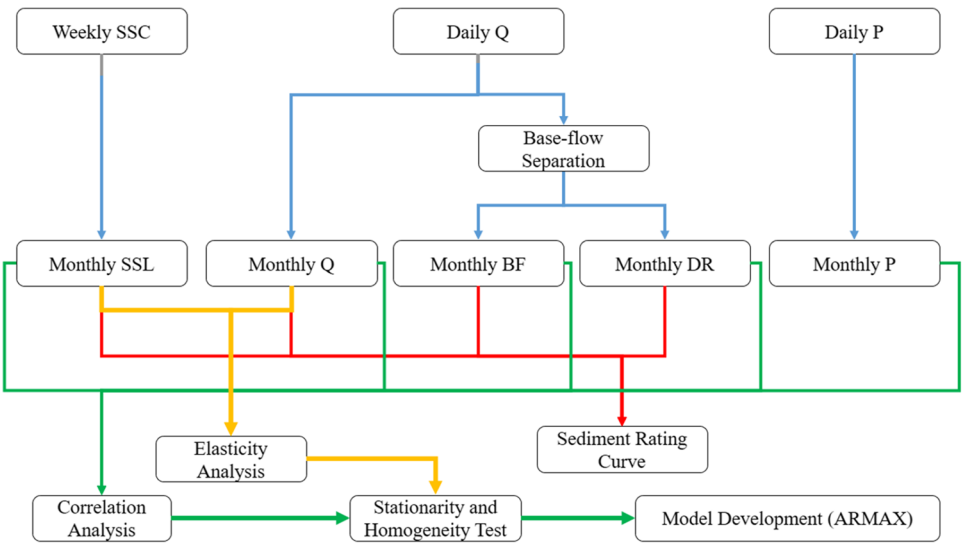

Fig. 3 Flowchart of the applied methodology

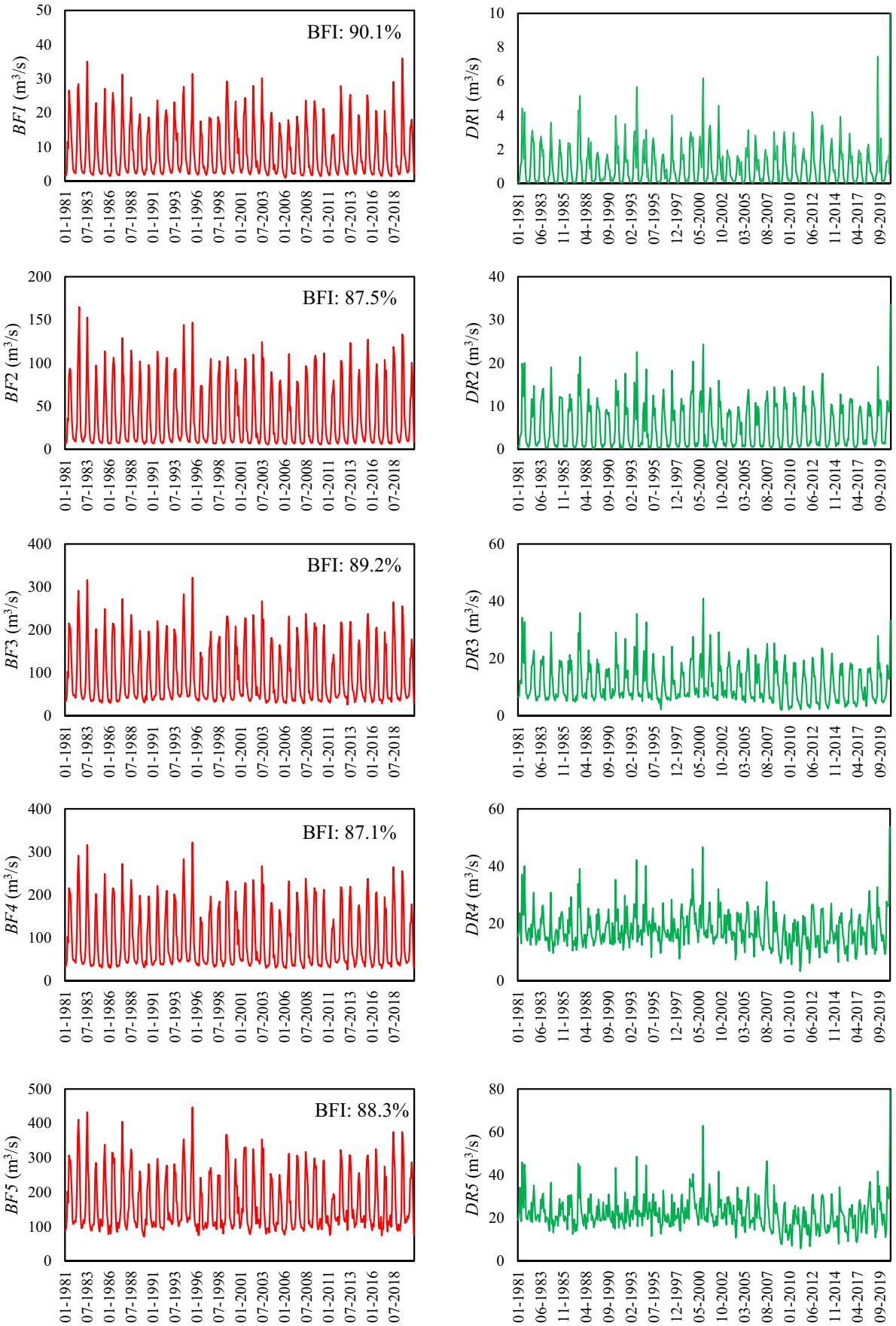
BFI: 90.1%
BF1 (m3/s)
DR1 (m3/s)
BFI: 87.5%
BF2 (m3/s)
DR2 (m3/s)
BFI: 89.2%
BF3 (m3/s)
DR3 (m3/s)
BFI: 87.1%
BF4 (m3/s)
DR4 (m3/s)
BFI: 88.3%
BF5 (m3/s)
DR5 (m3/s)
01-1981
07-1983
01-1986
07-1988
01-1991
07-1993
01-1996
07-1998
01-2001
07-2003
01-2006
07-2008
01-2011
07-2013
01-2016
07-2018
06-1983
11-1985
04-1988
09-1990
02-1993
07-1995
12-1997
05-2000
10-2002
03-2005
08-2007
01-2010
06-2012
11-2014
04-2017
09-2019

◂**Fig. 4** Time series of *DR* and *BF* in the selected stations (BFI, the base flow index as the percentage of ratio of *BF* to the *Q*)

precipitation, average discharge rates, and the monthly total suspended sediment concentration for the common time January 1981 to October 2020 (478 months).

Data analysis

The correlation analysis is conducted based on Pearson's correlation coefficient matrix applied to the ensemble of the time series. Therefore, the time series of precipitation, streamflow, and suspended sediment concentration are examined against each other to investigate the linear dependence between allocated time series. Similarly, the auto-correlation function (ACF) and the partial-auto-correlation function (PACF) of the individual time series are tested to conduct temporal analysis that is evaluated in the development of ARMAX models which is discussed broadly in the section "The mathematical simulation."

Finally, the sediment rating curve (SRC) as a conventional method in *SSC* analysis is used (Asselman 2000; Mohammadi et al. 2021). It empirically represents the non-linear exponential functional relationship between the *SSC* and *Q*. Several alternative equations for the SRC have been reported in the literature; however, the most widely used SRC relationship has a form of

$$SSC = aQ^b \tag{1}$$

where a and b are constant values obtained from the data. It has to be noticed that SRCs are developed in three shapes in this study, i.e., as a product of the *Q-SSC* relationship as well as the products of *DR-SSC* and *BF-SSC*.

The mathematical simulation

Initially, the elasticity analysis is used to examine the flexibility of the models, their clustering capabilities, and the rate of influence for each predictor in space. It is commonly used in management practices to reveal the share of each predictor on prediction with consideration to its magnitude and significance. For this, usually a log-linear regression is used, while the outcome of such analysis details if the relationship between dependent and independent variables is inelastic (when the obtained coefficient $|\alpha| < 1$, that the *SSC* has a small response to the variable), unit elastic (when $|\alpha| = 1$, that the *SSC* has an exact response with the variable), or elastic (when $|\alpha| > 1$, that the *SSC* is greatly under the influence of the variable). Interested readers may refer to Working (1943), Leser (1963), Intriligator et al. (1996), and Deaton and Muellbauer (1980a, b) for more details about the application of elasticity analysis in time series analysis. In this respect, the elasticity analysis is conducted between the time series of monthly *SSC* and monthly *Q* as the dependent and the independent variables, respectively. A simple log-linear elasticity regression can be determined as

$$log\left(SSC_t\right) = \beta + \sum \left(\alpha_i log\left(Q_t^i\right)\right) \tag{2}$$

in which the intercept β and coefficients α are the parameters of the regression and can be evaluated with a *t*-test which defines if the obtained value is statically significant or not (*t*-critical is ± 1.96 at 0.05 significance level). Thereby, the effect of a non-significant coefficient can be ignored in the analysis regardless of the sign and/or value obtained in the analysis.

On the other hand, the inconsistency and non-homogeneity associated with the variables could induce the hydrologic features to change over time (Salas et al. 1980). Therefore, it is suggested to check the stationarity and homogeneity of the applied hydro-climatic variables in advance (Salas et al. 1980; Wang et al. 2009; Vazifehkhah and Kahya 2019). For this, the time series of the applied variables are checked for stationarity and homogeneity using the Augmented Dickey-Fuller (ADF: Dickey and Fuller 1979) and Pettitt's (Pettitt 1979) tests respectively.

Then, the Autoregressive Moving Average eXogenous (ARMAX) method is used to evaluate a multi-variable stochastic model fit in the simulation of the desired relationship between *SSC*, *P*, *Q*, and *DR*. For this, the *SSC* in the river stream is examined for the source of *SSC* brought either by precipitation, direct runoff washouts, or the upstream glacier melt, snowmelt, or the channel erosion. For this, the ARMAX (p, q, b) consisting of order-p time lag (maximum 2 in this study), order-q moving average of residuals (maximum 2 in this study), and order-b variables depending on the amount of contributing independent variable (maximum 6 in this study based on the scenario) were proposed. In this respect, a related equation takes the form of

$$SSC_t = \sum_{k=1}^{b}\left(\beta_k x_t^k\right) + \sum_{j=1}^{p}\left(\phi_j SSC_{t-j}\right) - \sum_{j=1}^{q}\left(\theta_j \varepsilon_{t-j}\right) - \varepsilon_t \tag{3}$$

in which t stands for the time interval, β is the coefficient or intercept obtained for the kth exogenous input, ϕ is the coefficient of jth order auto-regressive term, θ is the jth order moving average of residual series, ε. Therefore, by considering a different combination of p, q, and b orders, different scenarios can be generated. Then, the performance of models is evaluated using Akaike information criterion (*AIC*) and the determination coefficient (R^2) defined as

$$AIC = Nln\left(\frac{N}{N-n-1}\right)\sigma_\varepsilon^2 + 2(n+1) \tag{4}$$

$$R^2 = \left(\frac{Covariance\left(SSC, \widehat{SSC}\right)}{\left(\sigma_{SSC}\right)\left(\sigma_{\widehat{SSC}}\right)} \right)^2 \quad (5)$$

in which n, N, and σ_ε are respectively the number of parameters in the model, number of datasets, and standard deviation of the residual series. The *AIC* defines the parsimoniousness of the model, while R^2 denotes the portion of the variance explained by the applied scenario.

Results

The following section details the results obtained in data analysis or model development as detailed in the flowchart (Fig. 3).

Correlation analysis

The correlation coefficients between all of the time series (i.e., *SSC*, *Q*, *P*, *DR*, *BF*) are obtained to evaluate the nature of the relationship between suspended sediment concentration (*SSC*) in Porte du Scex station (most downstream station) and total streamflow in the same station (*Q*5), Branson (*Q*4), Sion (*Q*3), Brig (*Q*2), and Reckingen (*Q*1) stations; direct runoff (*DR*5, *DR*4, *DR*3, *DR*2, *DR*1) and base-flow (*BF*5, *BF*4, *BF*3, *BF*2, *BF*1) in the aforesaid stations; and the precipitation (*P*) in the Aigle station (at downstream). The outcomes of the correlation analysis are in Fig. 5 which shows the *SSC* data in Porte du Scex is less correlated with the precipitation, while more correlated with total streamflow data over the applied stations (Fig. 1). The correlation coefficients between *SSC* and *Q* and *BF* (Fig. 5) are higher than *DR* on every station. On the other hand, it is seen that the correlation between *Q* and *BF* is higher than the correlation between *Q* and *DR* on every individual station. Likewise, it can be understood that the *BF* has a greater quota in total *Q* and the nature of the river is permanent being fed by the snowmelt and/or groundwater.

Sediment rating curves

The sediment rating curve between *SSC* at Porte du Scex station and streamflow in five stations (*Q*5, *Q*4, *Q*3, *Q*2, *Q*1), and the *SRCs* for *SSC* and direct runoff (*DR*5, *DR*4, *DR*3, *DR*2, *DR*1) and base flow (*BF*5, *BF*4, *BF*3, *BF*2, *BF*1) are developed (Fig. 6). The *SRC* for *SSC* and total streamflow data at Porte du Scex station (*Q*5) yields an R^2 of 0.73 demonstrating the high applicability of the *SRC* for the applied

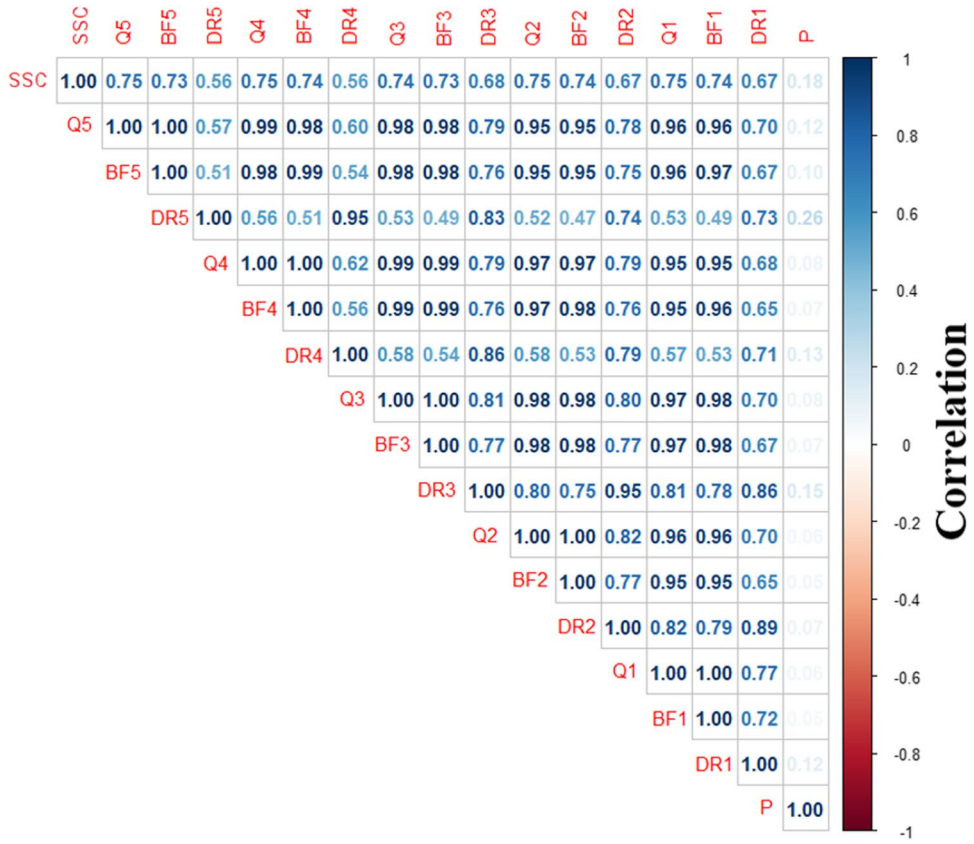

Fig. 5 The correlation matrix of all variables including P, SSC, Q, BF, and DR related to selected stations

cases. Developing the *SRCs* for *SSC* and streamflow at Branson, Sion, Brig, and Reckingen stations (*Q*4, *Q*3, *Q*2, *Q*1) shows that *SSC* has also a reasonable relationship between upstream streamflow which is more tangible for Sion, Brig, and Reckingen (*Q*3, *Q*2, *Q*1). In this regard, the relationships between the *SSC* and *Q*3, *Q*2, and *Q*1 are higher in contrast to the *Q*5 and *Q*4. Therefore, it may be interpreted as the effect of erosion occurring in the hillslope, human activities, glaciers, and/or snowmelt, etc., at the upstream of the river. It is seen that the *SSC* at Porte du Scex station has higher correlations with the *BF* and the *Q* compared to the *DR*. Similar to the results obtained for total streamflow, the *SRCs* established on *BF* for upstream stations give higher R^2 in comparison to the downstream stations. It is noteworthy that the incline of the rating curves increases from upstream (Porte du Scex, Fig. 6e) to downstream (Porte du Scex, Fig. 6a) indicating that the *Q* and the corresponding *BF* and *DR* have a higher effect on the *SSC* in the downstream.

Elasticity of the data

The elasticity analysis results are also given (Table 2) with a log transformation revealing that the *Q*5 (same as for the *SSC*) has the highest effect on the *SSC*. Based on the regression performance of the performed elasticity analysis, the model explains 98.6% of the total variance (R^2) in the *SSC* time series. For instance, a 1% change in *Q*5 causes in a 0.64% change in *SSC*. A similar association between *Q*4 and *SSC* can be observed while the *Q*1, *Q*3, and *Q*2 respectively have 0.59%, 0.58%, and 0.25% effects on the *SSC*. However, when the *t*-value is considered (Table 2), the *t*-value associated with *Q*1 exceeds 1.96 which indicates that the coefficients of elasticity obtained for *Q1* are significant, while the remaining coefficients are not statistically significant and could be ignored in the elasticity analysis. For instance, the *Q4* (Branson) owns a negative coefficient unlike the other stations, but due to the non-significant *t*-value it can be ignored or assumed with zero effect in the analysis.

As detailed above, the relationship between *SSC* and the predictors (*Q*1, *Q*2, *Q*3, *Q*4, and *Q*5) is quite inelastic, but it still interpreted about 99% of the variance which urges the need for detailed investigation about the micro-hydrology and morphology of the basin in future. In other words, it can be concluded that the changes in the *SSC* are extremely related to the discharge rates, but the portion and the direction the relationship may differ due to the micro- and macro-hydrological events at the basin. In this respect, the relationship between *SSC* and the streamflow in the river is found to be quite complicated and nonlinear that needs to be simulated with a deterministic-stochastic approach that interprets the effect of time and space, simultaneously.

The mathematical simulation

To develop Autoregressive Moving Average eXogenous (ARMAX) best-fit equations, different scenarios are developed. The urge for using these scenarios relies on the examination of the role of *DR*, *P*, and *Q* on the *SSC* (i.e., *BF* is not expected to be the source of *SSC* when it cannot be recognized as the streamflow when *DR* exists). Therefore, the most relevant variable sets in the form of suggested scenarios would reveal the most reliable scenario that is probably taking place. To this end, considering the obtained results (Table 2), the scenarios are suggested as follows:

$$SSC_t = f\left(SSC_{t-j}, \varepsilon_t, Q_t^5, P_t\right) \tag{6}$$

$$SSC_t = f\left(SSC_{t-j}, \varepsilon_t, Q_t^1, P_t\right) \tag{7}$$

$$SSC_t = f\left(SSC_{t-j}, \varepsilon_t, Q_t^1, Q_t^2, Q_t^3, Q_t^4, Q_t^5, P_t\right) \tag{8}$$

$$SSC_t = f\left(SSC_{t-j}, \varepsilon_t, DR_t^5, P_t\right) \tag{9}$$

$$SSC_t = f\left(SSC_{t-j}, \varepsilon_t, DR_t^1, P_t\right) \tag{10}$$

$$SSC_t = f\left(SSC_{t-j}, \varepsilon_t, DR_t^1, DR_t^2, DR_t^3, DR_t^4, DR_t^5, P_t\right) \tag{11}$$

to define if the *DR* or the *Q* (*BF* is the same as *Q* due to the permanent nature of the river and not likely to be an alternative source in the production of the suspended sediment concentration) reveals the most relevant results associated with the *SSC* while *j*th time lag and randomness ε either in moving average or random walk is considered at time *t*. In other words, the proposed scenarios investigate the effect of upstream (glacier-melt, snowmelt, channel erosion etc.), rainstorm washouts (at the downstream), dust brought by the immediate precipitation over the channel in the most downstream station, and the temporary deposition and/or motion of the sediment (lag times) on the total suspended sediment concentration at the Port du Scex station.

Since ARMAX uses autoregressive (AR) and moving average (MA) components for the *SSC*, the autocorrelation function (ACF; Fig. 7a) and partial autocorrelation function (PACF; Fig. 7b) of the *SSC* time series are applied to define the order of the AR and MA process in ARMAX models. Based on the analysis (Fig. 7), both AR and MA components exist while the nature of the phenomenon is based on the dragged sediment components before time *t* and also randomness like the phenomenon itself.

The combinations of models and scenarios are generated (Eqs. 6–11) to study the effect of *DR* or *Q* on the *SSC* (Fig. 8 and Table 3). The developed equations for the proposed scenarios are given as follows:

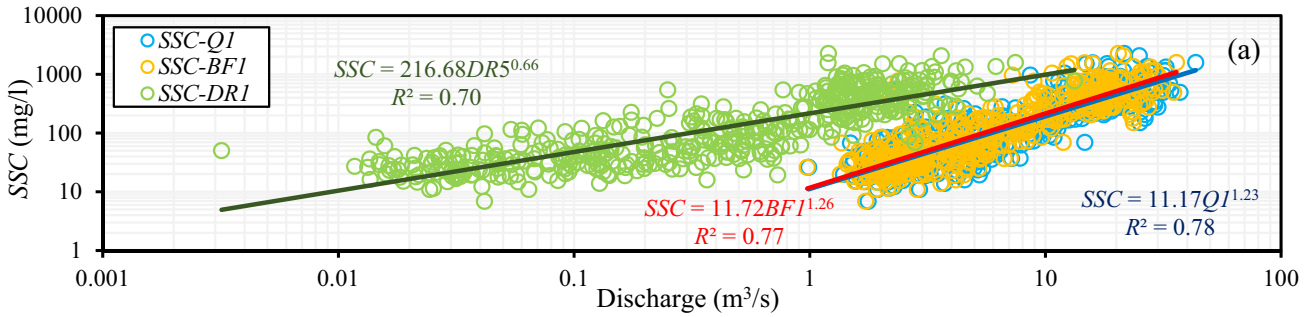
SSC-Q1
SSC-BF1
SSC-DR1
SSC = 216.68DR5^0.66
R² = 0.70
SSC = 11.72BF1^1.26
R² = 0.77
SSC = 11.17Q1^1.23
R² = 0.78
(a)
SSC (mg/l)
Discharge (m³/s)

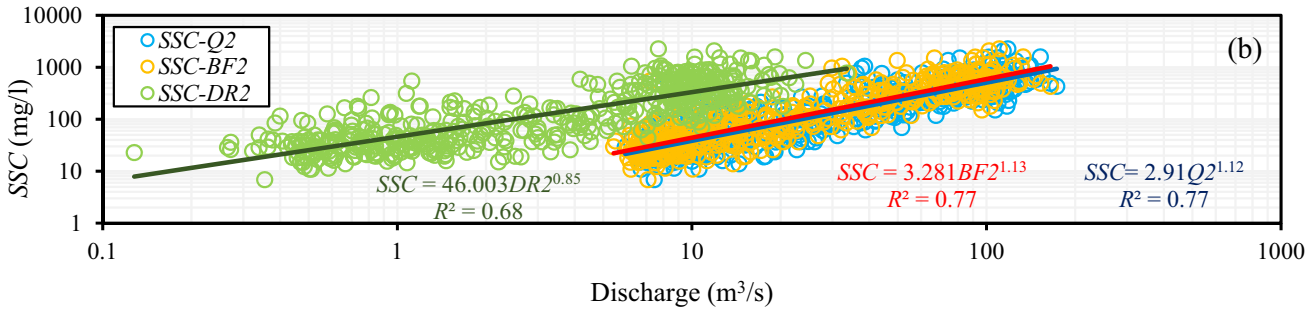
SSC-Q2
SSC-BF2
SSC-DR2
SSC = 46.003DR2^0.85
R² = 0.68
SSC = 3.281BF2^1.13
R² = 0.77
SSC= 2.91Q2^1.12
R² = 0.77
(b)
SSC (mg/l)
Discharge (m³/s)

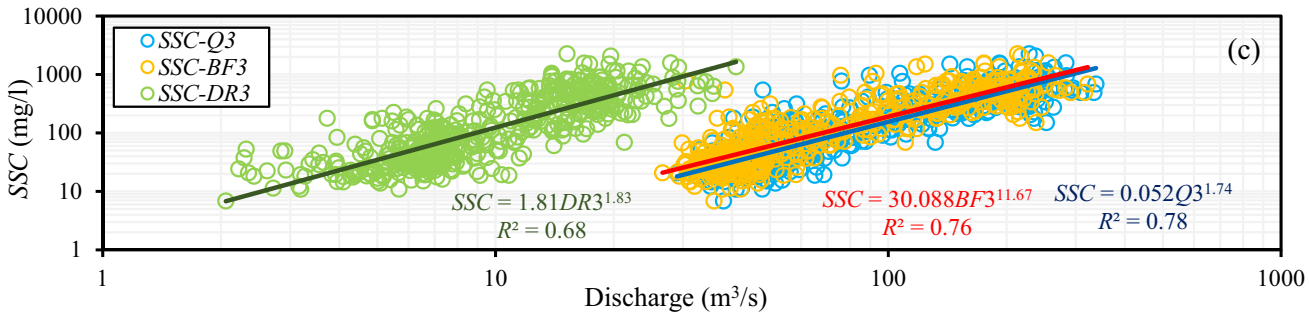
SSC-Q3
SSC-BF3
SSC-DR3
SSC = 1.81DR3^1.83
R² = 0.68
SSC = 30.088BF3^11.67
R² = 0.76
SSC = 0.052Q3^1.74
R² = 0.78
(c)
SSC (mg/l)
Discharge (m³/s)

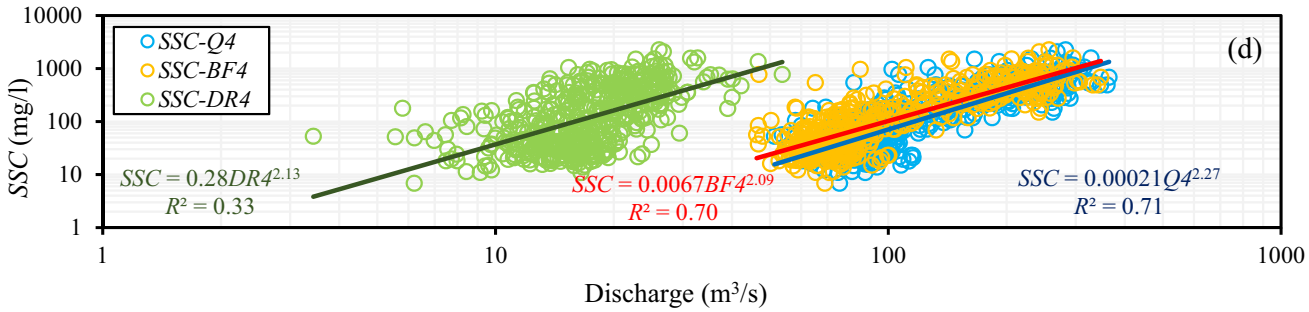
SSC-Q4
SSC-BF4
SSC-DR4
SSC = 0.28DR4^2.13
R² = 0.33
SSC = 0.0067BF4^2.09
R² = 0.70
SSC = 0.00021Q4^2.27
R² = 0.71
(d)
SSC (mg/l)
Discharge (m³/s)

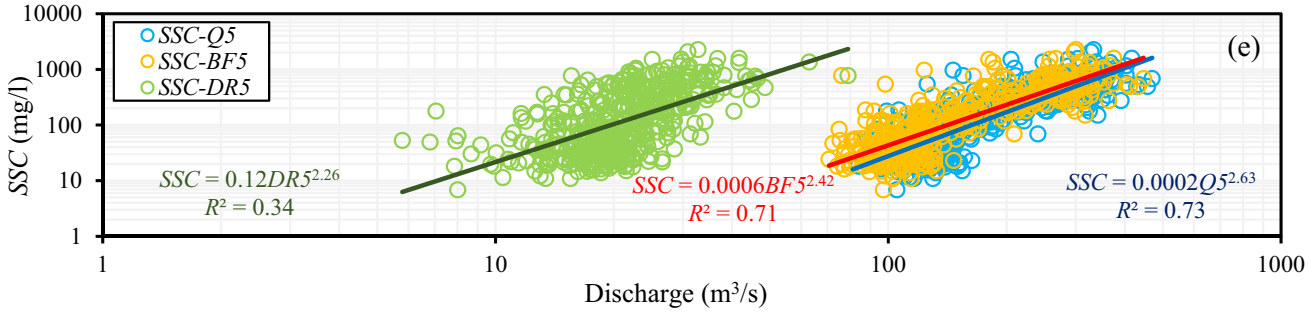
SSC-Q5
SSC-BF5
SSC-DR5
SSC = 0.12DR5^2.26
R² = 0.34
SSC = 0.0006BF5^2.42
R² = 0.71
SSC = 0.0002Q5^2.63
R² = 0.73
(e)
SSC (mg/l)
Discharge (m³/s)

◂**Fig. 6** Sediment rating curves related to suspended sediment concentration (*SSC*) at Porte du Scex station and *Q*, *BF*, and *DR* at (a) Reckingen, (b) Brig, (c) Sion, (d) Branson, and (e) Porte du Scex stations

$$SSC_t = \left(-317.598 + 2.771Q_t^5 + 0.869P_t\right) + \left(-0.352SSC_{t-1} + 0.263SSC_{t-2} + 0.622\varepsilon_{t-1} + \varepsilon_t\right) \quad (12)$$

$$SSC_t = \left(-86.790 + 27.776Q_t^1 + 1.209P_t\right) + \left(-0.293SSC_{t-1} + 0.549\varepsilon_{t-1} + 0.188\varepsilon_{t-2} + \varepsilon_t\right) \quad (13)$$

$$SSC_t = \left(-180.409 + 1.004Q_t^5 + 1.976Q_t^4 - 4.837Q_t^3 + 4.549Q_t^2 + 21.738Q_t^1 + 1.201P_t\right) + \left(-0.415SSC_{t-1} + 0.616\varepsilon_{t-1} + 0.192\varepsilon_{t-2} + \varepsilon_t\right) \quad (14)$$

$$SSC_t = \left(-106.305 + 13.795DR_t^5 + 0.946P_t\right) + \left(1.730SSC_{t-1} - 0.998SSC_{t-2} - 1.682\varepsilon_{t-1} + 0.951\varepsilon_{t-2} + \varepsilon_t\right) \quad (15)$$

$$SSC_t = \left(73.795 + 133.247Q_t^1 + 0.819P_t\right) + \left(-0.352SSC_{t-1} + 0.263SSC_{t-2} + 0.622\varepsilon_{t-1} + \varepsilon_t\right) \quad (16)$$

$$SSC_t = \left(-10.365 + 5.649DR_t^5 - 14.236DR_t^4 + 32.644DR_t^3 \pm 13.249DR_t^2 + 73.629DR_t^1 + 0.362P_t\right) + \left(0.565SSC_{t-1} - 0.299SSC_{t-2} - 0.1842\varepsilon_{t-1} + 0.229\varepsilon_{t-2} + \varepsilon_t\right) \quad (17)$$

According to the obtained results (Table 3) in terms of R^2 and *AIC*, the third scenario could be recognized as the best-fit scenario model. Hence, the time series of the best models obtained from the six scenarios are presented (Fig. 9), which shows their acceptable performances in capturing the sediment concentration in the river streams. However, some recent extremes in the *SSC* values exceeded the predictions. As also detailed previously (Fig. 8 and Table 3), such a model explains about 63% of the volatilities in the time series, while most of the deviations occurred due to outliers of the extreme events that could be probably in response to the high flows caused by the temperature increase and the sudden ice and/or snowmelts. What is more, and based on the obtained coefficients for the best model (Eq. 14), both of the exogenous variables (first parentheses of Eq. 14) and the stochastic variables (second parentheses of Eq. 14) alter the simulations. By considering the discharge rates in Eq. (14), the $Q1$ has the highest coefficient which also confirms the results of the elasticity analysis that were already explained (Table 2). Thereby, it could be interpreted that the most upstream parts of the URB are the main source (i.e., ice and snowmelt upstream) of the *SSC* at Rhone River, but the streamflow has a dominant effect against direct runoff in the production of *SSC* at the Port du Scex station. It is also concluded from the lower *P* coefficient that the best-fit model conceptualizes a non-significant effect of precipitation over the *SSC* at the Port du Scex station, which is in line with the correlation analysis results that were explained earlier. Alternatively, the weak relationship between the *SSC* and *DR* also emphasizes the less impact of the *P* (at Aigle) on the *SSC* (at Porte du Scex). For testing this hypothesis, temperature and precipitation time series at Grächen and Visp stations (located upstream of the URB) are compared with the *SSC*. In this respect, the correlation coefficients between *SSC* and temperature in Grächen and Visp stations respectively depict 0.66 and 0.65, while the correlations associated with precipitation in the same stations were respectively 0.26 and 0.20. Hence, the main source of the *SSC* in the upstream brought by *Q* is probably the glacier or snowmelt rather than rainfall washouts or dust brought by the precipitation. A similar result is obtained by the sediment rating curve in the Reckingen station which depicts a higher correlation with the *SSC* at the Porte du Scex station.

As given in the scatter plot below (Fig. 10), the observed values contain more outliers that could not be simulated by the models. However, other properties of the distribution including median, average, quartile ranges, minima, and maxima are preserved adequately. In this respect, the results of the model fit can be considered acceptable enough for further application.

Discussion

The suspended sediment concentration studies in rivers could provide valuable information about the source of sediment transport for theoretical and practical uses. The amount of sediment being transported through the Rhone River to Lake Geneva is about 500,000 tons and reaches up to almost five million tons per year (Loizeau and Dominik 2000), and therefore needs to be studied carefully to avoid probable hazards and damages to the infrastructure and the environment of the surrounding regions. The process of *SSC* transport into the Rhone River is a challenging issue in particular with the increase of extreme precipitation events and heatwaves. Although the most recent glacial cover in the URB is estimated to be around 11% (FOEN, 2021), the investigation of the *SSC* process in the mountainous URB which hosts some of the largest Alpine glaciers gains more importance. The hydrological regime of URB results in the rainfall-runoff interactions having a non-linear and complex mechanism. For instance, during the winter as the freezing level falls below 900 m above sea level for a long period where the mean altitude of the basin reaches up to 2100 m above sea level, snowfall is a dominant precipitation type. This fact is confirmed through the sediment rating curve and

Table 2 Elasticity analysis of the log-linear regression with R^2 0.986

Parameter	Coefficient	*t*-value
*Q*1	0.594	3.736
*Q*2	0.254	1.291
*Q*3	0.581	1.437
*Q*4	−0.636	−1.476
*Q*5	0.637	1.903

the performed data analysis where *SSC* has a higher correlation with the base flow rather than the direct runoff. The base flow could be recognized as the dominant contributor to the streamflow. Therefore, the source of *SSC* seems to be related to glacier or snowmelt, or channel erosion rather than washouts from the overland flow or the dust brought by the immediate precipitation. This hypothesis is then examined by comparing the *SSC* with temperature and precipitation time series at the Grächen and Visp stations in the upstream areas. Results denote that correlation between the *SSC* and temperature is more significant than the *SSC* and precipitation; and therefore, the source of *SSC* is more likely the ice, glacier, or snowmelt at the upstream of the river. In this respect, as the temperature rises in March–May, the number of rainfall events increases which is followed by the decrease in the snow cover area over the basin. So, the simultaneous increase in discharge driven by the snowmelt in the rivers and channels, and the ice melt from the glaciers as well as the increase in the erodible area under rainfall, results in the peak *SSC*s in June–July. Therefore, the major glaciers of the URB

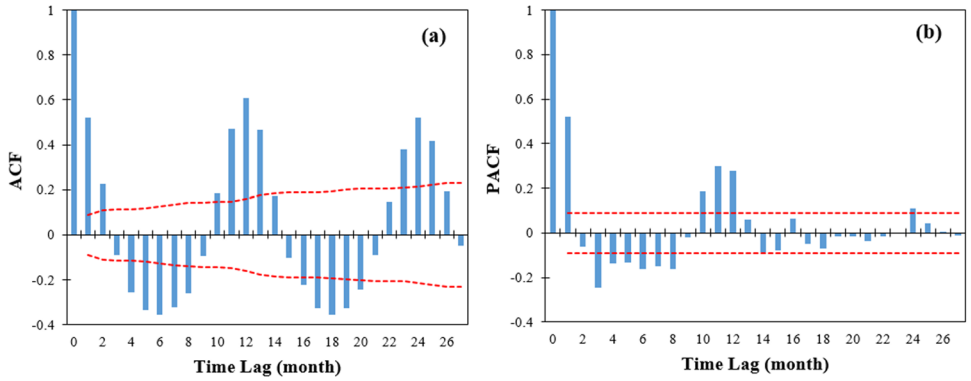

Fig. 7 The ACF and PACF related to *SSC* time series

Fig. 8 Time series of observation versus ARMAX model

Table 3 Results of the conducted models based on the scenarios given in Eqs. (12–17)

Scenario		Equation (12)	Equation (13)	Equation (14)	Equation (15)	Equation (16)	Equation (17)
ARMAX (1,0,*b*)	R^2	0.602	0.609	0.626	0.465	0.519	0.559
	AIC	6429.91	6420.93	6408.66	6571.76	6522.93	6487.16
ARMAX (1,1,*b*)	R^2	0.603	0.609	0.626	0.465	0.519	0.560
	AIC	6430.23	6422.73	6409.69	6573.76	6524.47	6488.83
ARMAX (1,2,*b*)	R^2	0.606	0.612	**0.629**	0.473	0.524	0.562
	AIC	6428.41	6421.67	**6408.09**	6568.16	6522.55	6488.71
ARMAX (2,0,*b*)	R^2	0.604	0.609	0.627	0.465	0.519	0.560
	AIC	6429.39	6422.61	6409.01	6573.75	6524.14	6488.68
ARMAX (2,1,*b*)	R^2	0.607	0.611	0.629	0.467	0.531	0.562
	AIC	6428.30	6422.90	6408.59	6573.38	6516.22	6489.52
ARMAX (2,2,*b*)	R^2	0.607	0.612	0.629	0.552	0.531	0.564
	AIC	6429.84	6423.66	6410.04	6496.30	6518.33	6489.32

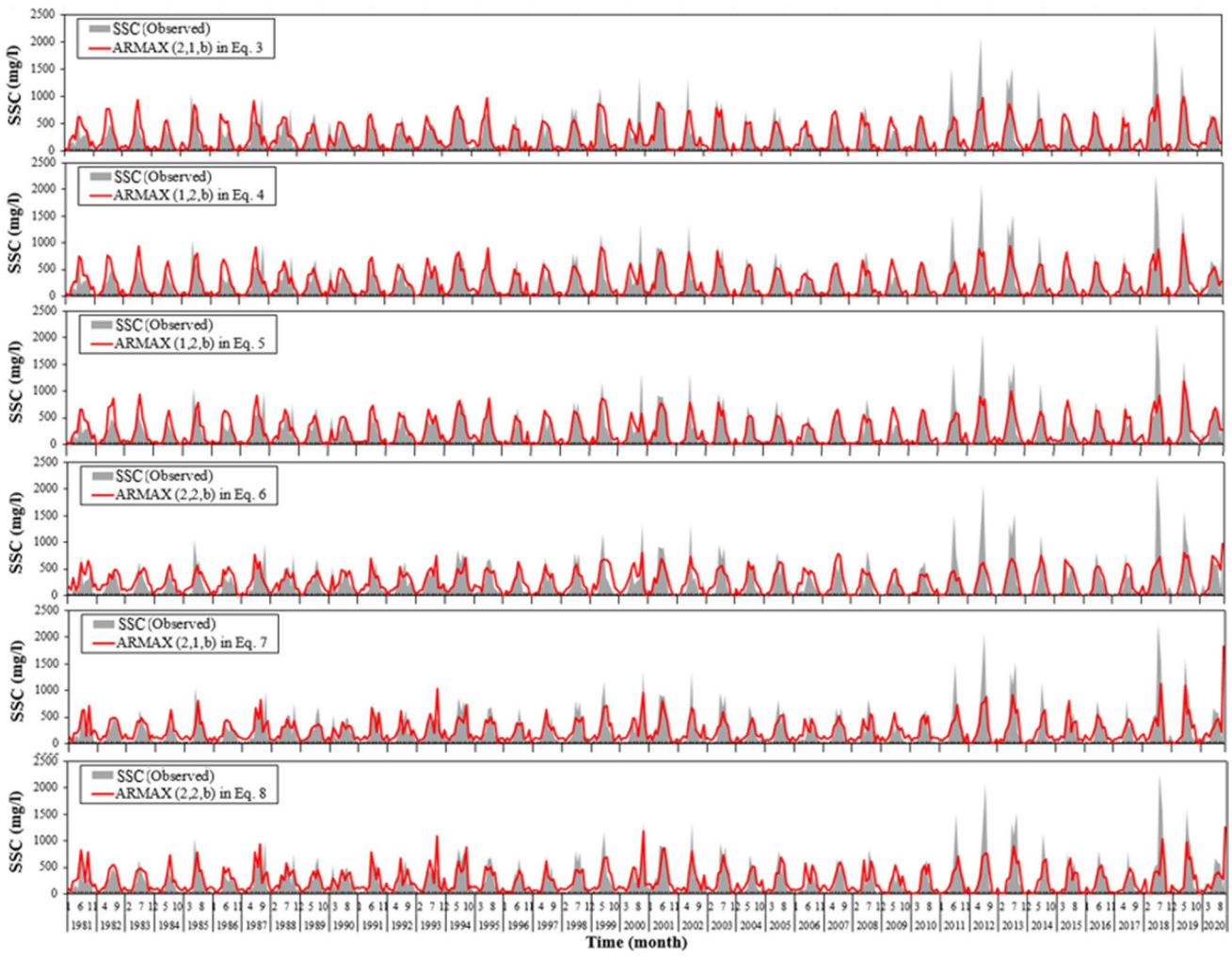

Fig. 9 The time series of the observed and the best-fit models

that are located upstream of the Reckingen and Brig stations are probably the main source of *SSC* to the river throughout the year. This was also emphasized by Costa et al. (2018b) who showed the role of glaciers on the upstream regions of

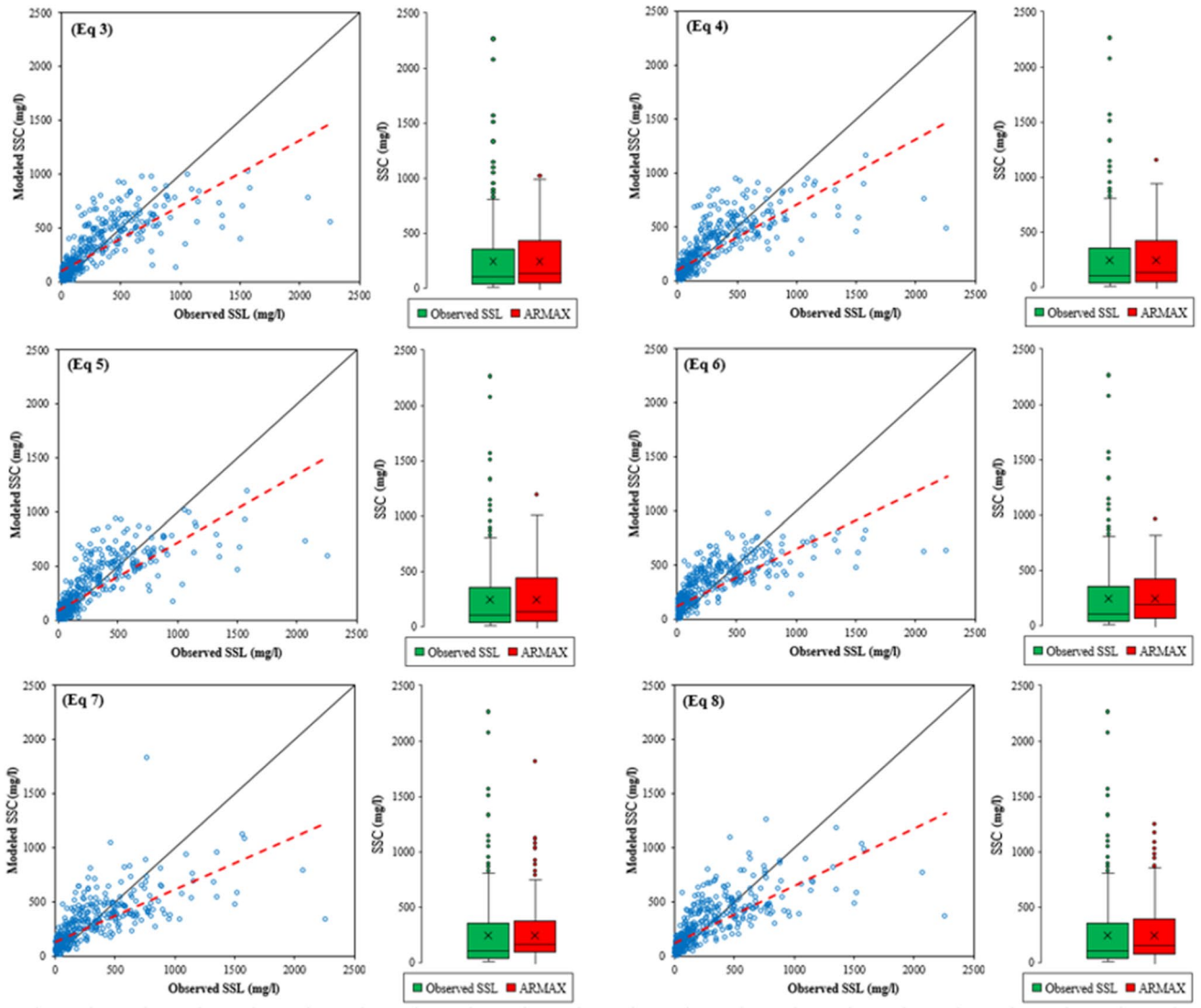

Fig. 10 Scatter plots and box-whiskers of the proposed best-fit models

the URB as the main suspended sediment contributors of the Rhone River. However, the considerable glaciers' existence in the URB and the amount of *SSC* which is contributed and being transferred to the main river through the current erosion in the small valleys and channels make the phenomenon very complex which needs to be studied through various time series analysis techniques and methods. Although the amount of precipitation decreases in August–September, the ice and snowmelt from glaciers continue to feed the Rhone River which keeps the *SSC* values significant until the autumn and enhance the significant relationship of *SSC* with the base flow (i.e., low flow) throughout the year. This phenomenon generates several extreme values resulting in the outliers in the *SSC* time series causing a negative impact on the performance of the proposed models.

In order to find the possible relationship between *DR* and *SSC*, the sliding interval approach is applied and then the *BF* and *DR* time series are analyzed together with *Q* in five stations. Furthermore, *P* in one station (most downstream station) is incorporated into the analysis to study its possible impact on *SSC*. Correlation analysis among the variables illustrates the higher correlation between the *SSC* at Porte du Scex station and not only streamflow in the same station but also streamflow in other four upstream stations where correlation coefficients between *SSC* and, *Q*5 and *Q*4 are found to be equal. But, the effect of *Q*1 (the most upstream station) on the *SSC* at Port du Scex station is higher than that of the remaining streamflows when *Q*5 (in the same station where *SSC* is measured) is neglected. This fact can be justified by the effect of erosion in the area

in which the considered sediment supply may be probably located upstream of the basin. It also confirms the findings of Schoch et al. (2018) who revealed the major contribution of glaciers on the upstream of the URB. Considering the relationship between the *BF* and *DR* with *SSC*, findings obtained in the *SRCs* analysis tend to support the correlation analysis results where, interestingly, the *SSC* is found more correlated to the *BF* (standing for the low flow through the year instead of *Q*) in contrast to the *DR*. It can also be linked to the nature of the Rhone River that is a permanent river and may be fed by alternative sources such as natural springs, groundwater, ice, and snowmelt. Alternatively, in permanent rivers such as the Rhone River, the base flow provides more water than direct runoff. Therefore, the continuous channel erosion, temporary deposition and motion of the sediments through the river stream, and geometry of the river result in a higher correlation coefficient between base flow, as stands for the largest portion of the streamflow, and the suspended sediment yield.

Conducted elasticity analysis shows that streamflow at Porte du Scex station (*Q*5) is the most important contributor among the selected variable that induces the *SSC* where changing 1% in *Q*5 quantity causes a 0.64% change in *SSC*. But interestingly, the *Q*1 was found to be the most significant source of *SSC* downstream. Relying on the correlation and elasticity analysis and ACF and PACF, six different scenarios are developed to construct the best-fit relationships for *SSC* computation by applying the ARMAX approach. Examination of different scenarios indicates that the scenarios which incorporate all upstream streamflow and precipitation variables generate better results. This agrees with foregone results that *SSC* in Porte du Scex station is greatly dependent on the upstream events rather than the most downstream station. The results of *SRC* and ARMAX models also revealed a stronger relationship between the discharge at Reckingen station (located upstream of the URB) and *SSC* at the Porte du Scex station (downstream of the URB). Eventually, it can be concluded that in total agreement with the previous studies that the source of suspended sedimentation are the upstream stations that gain water from glaciers and ice melt.

Conclusions

The following conclusions are made from the conducted analysis detailed above.

The effect of upstream events surpasses the effect of *DR* and direct precipitation over the river channel in the evaluation of the *SSC* at the most downstream station.

The temperature disturbances and the corresponding snow and ice melts upstream are likely to be the main source of *SSC* downstream, while the effect of channel erosion or bedded sediment is not clear. The morphology of the study area may support the finding where the largest Alpine glaciers exist in the URB.

The applied ARMAX models are capable of interpreting the relationship between *SSC*, *DR*, *P*, and *Q* while a similar application is suggested for further investigation. The models with more flexible and consistent behavior against extreme values, seasonality, and outliers would present a robust performance.

Overall, our results showed that future studies must incorporate the effect of glaciers and their retreat in suspended sediment concentration due to global warming which challenges the analysis process in the URB.

Acknowledgements We acknowledge the Federal Office of Meteorology and Climatology of Switzerland (MeteoSwiss) for making available the Precipitation data. We also thank the Hydrology Division of the Federal Office for the Environment (FOEN), Switzerland, for making available the discharge and suspended sediment data.

Author contribution The author contributions are listed as follows:
Mir Jafar Sadegh Safari, Saeed Vazifehkhah, Babak Vaheddoost: Conceptualization.
Saeed Vazifehkhah, Babak Vaheddost: Data curation.
Babak Vaheddoost, Mir Jafar Sadegh Safari: Formal analysis.
Mir Jafar Sadegh Safari, Babak Vaheddoost, Saeed Vazifehkhah: Investigation.
Babak Vaheddoost, Mir Jafar Sadegh Safari: Methodology.
Saeed Vazifehkhah, Babak Vaheddoost: Resources.
Babak Vaheddoost: Software.
Mir Jafar Sadegh Safari: Supervision.
Mir Jafar Sadegh Safari, Saeed Vazifehkhah, Babak Vaheddoost: Validation.
Mir Jafar Sadegh Safari, Saeed Vazifehkhah, Babak Vaheddoost: Visualization.
Saeed Vazifehkhah, Babak Vaheddoost, Mir Jafar Sadegh Safari: Writing – original draft.
Mir Jafar Sadegh Safari, Saeed Vazifehkhah, Babak Vaheddoost: Writing – review and editing.

Data availability The datasets used and/or analyzed during the current study are available from the corresponding author on reasonable request.

Declarations

Ethics approval and consent to participate Not applicable.

Consent for publication Not applicable.

Competing interests The authors declare no competing interests.

References

Andrews ED (1980) Effective and bankfull discharges of streams in the Yampa River basin, Colorado and Wyoming. J Hydrol 46(3):311–330. https://doi.org/10.1016/0022-1694(80)90084-0

Asselman NEM (2000) Fitting and interpretation of sediment rating curves. J Hydrol 234(3–4):228–248

Costa A, Molnar P, Stutenbecker L, Bakker M, Silva TA, Schlunegger F, Girardclos S (2018a) Temperature signal in suspended sediment export from an Alpine catchment. Hydrol Earth Syst Sci 22(1):509–528. https://doi.org/10.5194/hess-22-509-2018

Costa A, Anghileri D, Molnar P (2018b) Hydroclimatic control on suspended sediment dynamics of a regulated Alpine catchment: a conceptual approach. Hydrol Earth Syst Sci 22(6):3421–3434. https://doi.org/10.5194/hess-22-3421-2018

Dabrin A, Bégorre C, Bretier M, Dugué V, Masson M, Le Bescond C, Coquery M (2021) Reactivity of particulate element concentrations: apportionment assessment of suspended particulate matter sources in the Upper Rhône River. France J Soils Ad Sediments 21(2):1256–1274. https://doi.org/10.1007/s11368-020-02856-0

Deaton, A. & Muellbauer J. 1980a. An almost ideal demand system. Am Econ Rev 70.

Deaton A, Muellbauer J (1980) Economics and consumer behaviour. UK, Cambridge University Press, Cambridge

Dickey DA, Fuller WA (1979) Distribution of the estimators for autoregressive time series with a unit root. J Am Stat Assoc 74:423–431

Esteves M, Legout C, Navratil O, Evrard O (2019) Medium term high frequency observation of discharges and suspended sediment in a Mediterranean mountainous catchment. J Hydrol 568:562–574. https://doi.org/10.1016/J.JHYDROL.2018.10.066

Frings RM, Kleinhans MG (2008) Complex variations in sediment transport at three large river bifurcations during discharge waves in the river Rhine. Sedimentology 55:1145–1171. https://doi.org/10.1111/j.1365-3091.2007.00940.x

Harun, M. A., Safari, M. J. S., Gul, E., & Ab Ghani, A. (2021). Regression models for sediment transport in tropical rivers. Environ Sci Pollut Res 1–19.

Han J, Gao J, Luo H (2019) Changes and implications of the relationship between rainfall, runoff and sediment load in the Wuding River basin on the Chinese Loess Plateau. CATENA 175:228–235. https://doi.org/10.1016/j.catena.2018.12.024

Intriligator, M., Bodkin, R. & Hsiao, C. (1996). Application to households; demand analysis. In Econometric models, techniques, and applications. New Jersey, USA, Prentice-Hall.

Jain, S.K. (2001). Development of integrated sediment rating curves using ANNs. J. Hydraulic Eng., ASCE 127 (1), 30–37. https://doi.org/10.1061/(ASCE)0733-9429 (2001)127:1(30).

Kisi O, Yaseen ZM (2019) The potential of hybrid evolutionary fuzzy intelligence model for suspended sediment concentration prediction. CATENA 174:11–23. https://doi.org/10.1016/j.catena.2018.10.047

Klein, A. (2016) Les apports par les affluents au Leman et au Rhone a l'aval du Geneve et leur qualite. Rapp. Comm. int. prot. eaux Leman contre pollut., Campagne 2015, 2016, 108–114, Lausanne.

Leser CE (1963) Forms of Engel functions. Econometrica 31:694–703

Loizeau J-L, Dominik J (2000) Evolution of the Upper Rhone River discharge and suspended sediment load during the last 80 years and some implications for Lake Geneva. Aquat Sci 62(1):54–67. https://doi.org/10.1007/s000270050075

Loizeau JL, Girardclos S, Dominik J (2012) Taux d'accumulation de sediments recents et bilan de la matiere particulaire dans le Lema (Suisse - France). Arch Des Sci 65:81–92

Martinez JM, Guyot JL, Filizola N, Sondag F (2009) Increase in suspended sediment discharge of the Amazon River assessed by monitoring network and satellite data. CATENA 79:257–264. https://doi.org/10.1016/j.catena.2009.05.011

Meshram SG, Safari MJS, Khosravi K, Meshram C (2021) Iterative classifier optimizer-based pace regression and random forest hybrid models for suspended sediment load prediction. Environ Sci Pollut Res 28(9):11637–11649

Mohammadi, B., Guan, Y., Moazenzadeh, R., Safari, M. J. S. (2021). Implementation of hybrid particle swarm optimization-differential evolution algorithms coupled with multi-layer perceptron for suspended sediment load estimation. Catena, 198, 105024.

Pettitt AN (1979) A non-parametric approach to the change point problem. J R Stat Soc: Ser c: Appl Stat 28:126–135

Restrepo JC, Orejarena RAF, Torregroza AC (2017) Suspended sediment load in northwestern South America (Colombia): a new view on variability and fluxes into the Caribbean Sea. J South Am Earth Sci 80:340–352. https://doi.org/10.1016/j.jsames.2017.10.005

Safari, M. J. S. (2020). Hybridization of multivariate adaptive regression splines and random forest models with an empirical equation for sediment deposition prediction in open channel flow. J Hydrol 590, 125392.

Salas JD, Delleur V, Yevjevich V, Lane WL (1980) Applied modelling of hydrologic time series. Water Resources Publication, Chelsea, Michigan, USA

S Samadianfard K Kargar S Shadkani et al 2021 Hybrid models for suspended sediment prediction: optimized random forest and multi-layer perceptron through genetic algorithm and stochastic gradient descent methods Neural ComputAppl https://doi.org/10.1007/s00521-021-06550-1

Schoch A, Blöthe JH, Hoffmann T, Schrott L (2018) Multivariate geostatistical modeling of the spatial sediment distribution in a large scale drainage basin, Upper Rhone, Switzerland. Geomorphology 303:375–392. https://doi.org/10.1016/j.geomorph.2017.11.026

Shadkani S, Abbaspour A, Samadianfard S et al (2021) Comparative study of multilayer perceptron-stochastic gradient descent and gradient boosted trees for predicting daily suspended sediment load: the case study of the Mississippi River, U.S. Int J Sediment Res 36:512–523. https://doi.org/10.1016/j.ijsrc.2020.10.001

Shojaeezadeh SA, Nikoo MR, McNamara JP et al (2018) Stochastic modeling of suspended sediment load in alluvial rivers. Adv Water Resour 119:188–196. https://doi.org/10.1016/j.advwatres.2018.06.006

Sloto, R.A., and Crouse, M.Y. (1996). HYSEP: a computer program for streamflow hydrograph separation and analysis. U.S. Geological Survey, Water-Resources Investigations, Report 96–4040, Pennsylvania, 46 p.

Sok T, Oeurng C, Kaing V et al (2021) Assessment of suspended sediment load variability in the Tonle Sap and Lower Mekong Rivers. Cambodia Catena 202:105291. https://doi.org/10.1016/j.catena.2021.105291

Stutenbecker L, Delunel R, Schlunegger F, Silva TA, Šegvić B, Girardclos S, Christl M (2018) Reduced sediment supply in a fast eroding landscape? A multi-proxy sediment budget of the upper Rhône basin, Central Alps. Sed Geol 375:105–119. https://doi.org/10.1016/j.sedgeo.2017.12.013

Swiss Federal Office of the Environment (FOEN). Hydrological Data and Forecasts, https://www.hydrodaten.admin.ch/en

Tian S, Xu M, Jiang E, Wang G, Hu H, Liu X (2019) Temporal variations of runoff and sediment load in the upper Yellow River, China. J Hydrol 568:46–56. https://doi.org/10.1016/J.JHYDROL.2018.10.033

Vaheddoost B, Aksoy H (2018) Interaction of groundwater with Lake Urmia in Iran. Hydrol Process 32(21):3283–3295. https://doi.org/10.1002/hyp.13263

Vazifehkhah, S., & Kahya, E. (2019). Hydrological and agricultural droughts assessment in a semi-arid basin: inspecting the teleconnections of climate indices on a catchment scale. Agric Water Manag 217(April 2018), 413–425. https://doi.org/10.1016/j.agwat.2019.02.034

Walker, N., & Adele B. Hammack. (2000). Impacts of winter storms on circulation and sediment transport: Atchafalaya-Vermilion Bay Region, Louisiana, U.S.A. Journal of Coastal

Research, 16(4), 996–1010. Retrieved August 12, 2021, from http://www.jstor.org/stable/4300118

Wang H, Yang Z, Wang Y, Saito Y, Liu JP (2008) Reconstruction of sediment flux from the Changjiang (Yangtze River) to the sea since the 1860s. J Hydrol 349(3–4):318–332. https://doi.org/10.1016/j.jhydrol.2007.11.005

Wang H, Lin X, Qian L (2009) Crytic period analysis model of hydrological process and its application. Hydrol Process 23(13):1834–1843. https://doi.org/10.1002/hyp.7313

Working H (1943) Statistical laws of family expenditure. J Am Stat Assoc 33:43–56

Yang Z, Ji Y, Bi N, Lei K, Wang H (2011) Sediment transport off the Huanghe (Yellow River) delta and in the adjacent Bohai Sea in winter and seasonal comparison. Estuar Coast Shelf Sci 93(3):173–181. https://doi.org/10.1016/j.ecss.2010.06.005

Zakwan M, Pham QB, Zhu S (2021) Effective discharge computation in the lower Drava River. Hydrol Sci J 66(5):826–837. https://doi.org/10.1080/02626667.2021.1900853